

Field Study

Measurement of nanoparticle exposure in crematoriums and estimation of respiratory deposition of the nanoparticles by number and size distribution

Nobuyuki Kato¹, Yasuto Mastui², Masaki Takaoka^{1,3} and Minoru Yoneda¹

¹Department of Environmental Engineering, Graduate School of Engineering, Kyoto University, Japan, ²Agency for Health, Safety and Environment, Kyoto University, Japan and ³Department of Global Ecology, Graduate School of Global Environmental Studies, Kyoto University, Japan

Abstract: Objectives: Nanoparticles (NPs), including hazardous substances, are generated in crematoriums due to the high temperatures during the combustion process. NPs are reported to greatly impact animals' health by reaching the alveoli and being carried to the entire body through the blood stream. However, studies in crematoriums have yet to assess workers' exposure to the generated NPs. The purpose of this study is to assess workers' exposure to NPs released in crematoriums. **Methods:** Field surveys were conducted in three crematoriums with an emphasis on cremation, bone rearrangement and cleaning processes. The NP concentrations and size distributions were analyzed. The deposition of NPs in each respiratory region during each working process was calculated based on the measured data using the Human Respiratory Tract Model. **Results:** The mean particle number concentration was maximized momentarily during the bone rearrangement process. The concentration at the time a crematory's door was opened was 500,000 particle/cm³. NPs aggregated to micro-sized particles within a few minutes, dust generated by the bone rearrangement, or both. As a result of model calculation, the mean ratios (alveolar per the other regions by a crematory) were approximately 3.0 (bronchus and bronchioles regions: except for the first survey in crematorium A which had the obstruction of measurement) and 4.3 (extrathoracic airways). The ratios were similar for all crematoriums. **Conclusions:** These results can be used for health risk assessments in crematoriums. In addition,

these results should be applicable to estimate the inhalation unit risk of each respiratory organ such as lungs and nose.

(J Occup Health 2017; 59: 572-580)

doi: 10.1539/joh.17-0008-FS

Key words: Crematorium, Exposure assessment, Human Respiratory Tract Model, Nanoparticle, Risk assessment

Introduction

The number of crematoriums has increased globally in the past few decades^{1,2}. In particular, the death population of Japan is increasing every year and reached 1.3 million deaths per year as of 2015 (total death population, including still-born infants). Atmospheric pollution from crematoriums is becoming more serious: the cremation ratio in Japan is approximately 99.9%³. The studied pollutants are mainly polychlorinated dibenzo-p-dioxins and dibenzofurans (PCDD/Fs)^{4,6}, heavy metals (especially mercury released from amalgam fillings in teeth⁷⁻¹¹), combustion gases (NO_x, SO_x, CO, HCl), and particulate matter (PM)¹²⁻¹⁵. Soot dust produced during cremation includes the abovementioned substances.

The concentration range of PCDD/Fs depends greatly on the cremation condition¹. Takeda et al. studied the PCDD/F concentrations in the stack flue gas at 17 crematoriums in Japan. Total concentrations (normalized by 12% oxygen) of PCDD/Fs had a range of 4.9-1200 ng/Nm³ and 0.064-24 ng TEQ/Nm³⁵. Wang et al. showed the mean PCDD/F emissions (11% oxygen) from the stacks of two crematoriums in southern Taiwan were 2.36 (without a bag filter) and 0.322 ng TEQ/Nm³ (with a bag filter)⁶.

Focusing on the PM, mercury, and acidic gas released from conventional crematoriums in Japan, the reported peak

Received January 17, 2017; Accepted August 1, 2017

Published online in J-STAGE October 7, 2017

Correspondence to: N. Kato, Work Environment Research Group, National Institute of Occupational Safety and Health, Japan, 6-21-1 Nagao, Tama-ku Kawasaki, 214-8585, Japan (e-mail: kato@h.jiniosh.johas.go.jp)

proportion was 200-300 nm particles. The PM_{2.5} concentration ranged from 44.5 to 72.2 mg/Nm³ (12% oxygen). The arithmetic mean concentrations of HCl, SO₂, and mercury in flue gas without a bag filter and catalytic device were 61.3 mg/Nm³, 12.3 ppmv, 10.3 µg/Nm³ (T-Hg), and 8.19 µg/Nm³ (Hg⁰) (n = 103)¹⁴, respectively. The mean concentrations released from crematoriums equipped with these devices were 34.1 mg/Nm³, 11.5 ppmv, 4.5 µg/Nm³ (T-Hg), and 1.42 µg/Nm³ (Hg⁰) (n = 106). The results showed that these device could reduce the concentration of acidic compounds. While, it reported that dust ranged mainly on the nanoscale blow PM_{2.5} was generated from crematoriums¹⁵.

It is also reported that hexavalent chromium is eluted from the stainless steel casket-placement table during the cremation process¹². The cremation temperature increases above 800°C using oil and natural gas. Mercury is highly volatile, but mercury derived from dental amalgams is unstable at cremation temperatures (650°C-700°C)^{16,17}. The total PM concentration was 1.0-2.4 mg/m³, and the mercury concentration in PM was 0.005-0.300 mg/m³¹⁸.

A UK study on occupational exposure to individual workers in crematoriums is well known¹⁹. It found that the amount of mercury detected in the hair of workers exposed to mercury in crematoriums was unexpectedly lower compared with that detected in the hair of persons with occupational exposure to mercury in other workplaces. However, it is insufficient to consider only this study. A different study reported that nanoparticles (NPs) greatly impact rats because NPs reach the alveoli and are distributed throughout the body by blood²⁰. This impact depends on the particle diameter²¹. Because these results have potentially hazardous health effects on humans, an assessment of NPs and micron-sized particles in crematoriums on workers is important. However, no study has assessed crematorium workers' exposure to generated NPs in terms of particle diameter and concentration during each working process.

This study aims to clarify the concentrations of generated NPs during the working processes and assess the exposure to NPs using a respiratory deposition model. The maximum NP concentration and size distribution during different stages of the working process were analyzed. The initial values for the respiratory deposition model were obtained by the particle number concentration measured using a real-time monitoring apparatus. The exposure ratio for each respiratory region was calculated using the model. These results can be used for risk assessment of respirable particles released in crematoriums.

Methods

Field surveys were conducted in three crematoriums (A, B, and C). One (crematorium A) was surveyed twice. During each survey, the size and number concentration of

PM were measured during the working processes throughout the day. Fig. 1 shows the outline of the crematoriums and set points of each device. To obtain a comprehensive data of PM, real-time monitoring of airborne PM was conducted using a Scanning Mobility Particle Sizer (SMPS; Model 3910, TSI Inc.), an Optical Particle Sizer (OPS; Model 3330, TSI Inc.), and a Fast Mobility Particle Sizer (FMPS; Model 3091, TSI Inc.). The height of each measurement point was approximately 1 m. SMPS had running conditions of a flow rate at 0.8 l/min and scanned particles with diameters ranging from 10 to 300 nm in 60-second intervals. OPS had a flow rate of 1 l/min and scanned particles with diameters of 0.3-10 µm in 10-second intervals. FMPS, which was used only in crematorium C, had a flow rate of 10 l/min and scanned particles with diameters of 5.6-300 nm in 1-second intervals. The apparatuses were numbered in the order of the measurements. Crematoriums were equipped with a casket-placement table. The measurements were conducted around the casket-placement table using the aforementioned devices.

Crematorium C had the latest pressure control system. Consequently, it is expected to have the lowest exposure. A Low volume Pressure Impactor (LPI; LP-20, Tokyo Dylec, flow rate of 20 l/min) was used to collect airborne 130-nm (50% cutoff) PM, which is close to the peak diameter on the filter for the Scanning Electron Microscope (SEM) observations during the working processes. A glass fiber filter (T60A20, SIBATA) was used as the collecting filter.

Table 1 overviews the working processes and measurement apparatuses. In Japan, there are three main working processes: 1. operating the crematory (cremation), 2. bone rearrangement before inurnment, and 3. cleaning after inurnment. After cremation, the door of the crematory is opened, after which the casket-placement table comes out and bone rearrangement is performed. Depending on the crematorium, inurnment may be conducted without bone rearrangement. Each crematorium in Japan uses their own procedures for the working processes.

Crematorium B conducted inurnment directly without a bone rearrangement process. In addition, the remaining ashes and bone on the casket-placement table were cleaned on the following day prior to the next operation. All surveyed crematoriums had the same cremation time (approximately 50 min) and cooling time (10 min). However, the times for all other processes varied. The combustion temperature of the cremation ranged from 800°C to 950°C. In crematorium C, after the temperature of the crematory dropped below 100°C, the crematory's door was opened and the bone rearrangement process started. The bone rearrangement and cleaning processes were 20 min each in crematorium A, but less than 10 min in crematorium C. In crematorium B, only the cleaning process was conducted for 20 min. In all the crematoriums, the

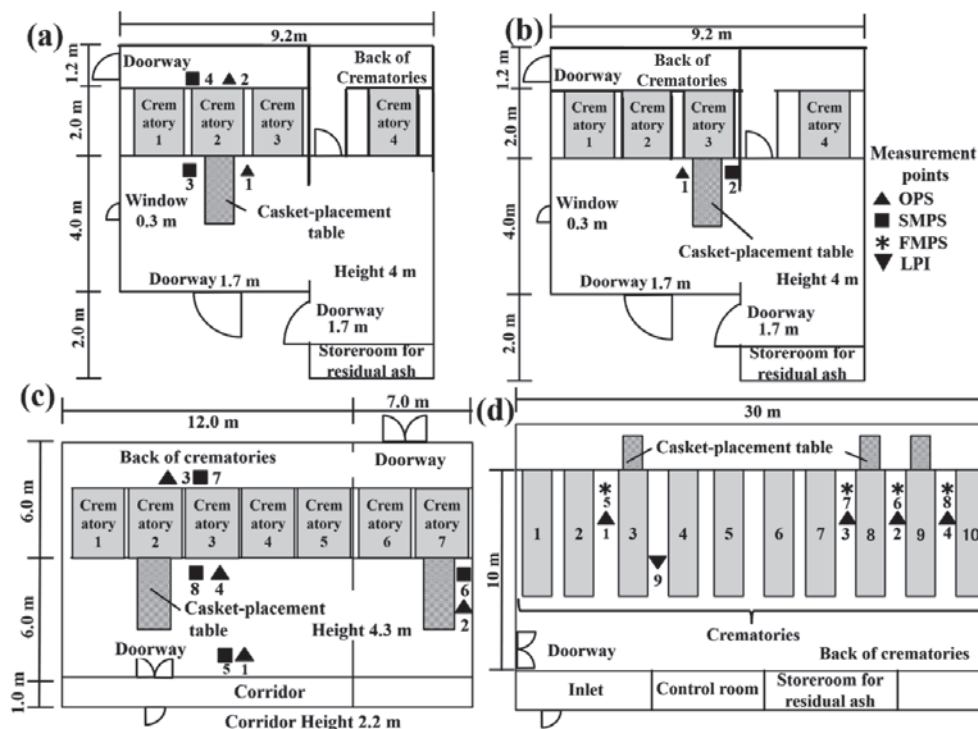


Fig. 1. Outline of the four surveyed crematoriums denoting approximate positions of processes and measurement locations of mobile apparatuses. (a) Crematorium A layout in the first field survey, (b) crematorium A layout in the second field survey, (c) crematorium B, and (d) crematorium C.

workers worked at the back of crematoriums during cremation, then around the casket-placement table during the bone rearrangement and cleaning processes.

PM characterization via SEM observations

To obtain the shape, size, and composition of the PM, a morphological observation was performed. The sampled filters were cut into pieces of approximately 5×5 mm. The cut pieces were fixed onto sample stages with carbon tape. To avoid charging the filters, the samples were sputtered with platinum-palladium and observed using SEM (JSM-5610, JEOL). SEM was equipped with Energy Dispersive X-ray Spectroscopy (EDS; JED-2300, JEOL). The acceleration voltage was 15.0 kV. To compare with the original condition, a blank filter was prepared. To check the components of the collected PM, elemental mapping and spectra analysis of the PM counts divided by the blank filter's counts were conducted using EDS.

Real-time measurements of the particle number concentration in each process

Real-time monitoring was conducted using SMPS for crematoriums A and B (FMPS for crematorium C). The OPS was operated for all the processes in all crematoriums. The particle number concentrations measured near each operation point were compared to the concentration measured for each working process in other crematori-

ums. When the crematorium's door was opened, it was predicted that the generated and accumulated particles during the cremation were released from the crematorium by thermal convection. Therefore, the analysis focused on the real-time monitoring of exposure at the time the crematorium's door is opened (crematorium 2 in Fig. 1a and crematorium 3 in Fig. 1b).

Respiratory deposition assessment

In this study, the deposition number of PM in the respiratory organs during the working processes was estimated using the International Commission on Radiological Protection (ICRP) Model²². The respiratory regions are divided into two regions (extrathoracic and tracheobronchial airways). Extrathoracic airways are further separated into two sub-regions (anterior nasal (ET_1), nasopharynx and larynx (ET_2)). The tracheobronchial airway is further separated into three regions (bronchus (BB), bronchioles (bb), and alveolar-interstitial). These five parts of the respiratory regions are assumed to be air filters with have unique deposition ratios and volumes. A total of nine filters are composed from these five regions (from inhalation to exhalation). The deposition at each respiratory region was calculated using this model and the parameters based on the workers in crematoriums (adult male, light work (such as cleaning), and nasal breathing). The calculations were conducted based on the measured

Table 1. Time course of each working process and measurement apparatus used. (a) Crematorium A layout in the first field survey, (b) crematorium A in the second field survey, (c) crematorium B, and (d) crematorium C.

(a)				(b)			
Time	Process	OPS	SMPS	Time	Process	OPS	SMPS
11:25	Before cremation	↑ 1	↑ 3	10:00	Before cremation	↑ 1	↑ 2
11:35		↓ 2	↓ 4	10:10			
11:50	Crematory No.2 in operation	↑	↑	10:20	Crematory No.3 in operation	↑ 1	↑ 2
14:30				10:30			
14:40	Bone rearrangement before inurnment No.2	↑ 2	↑ 4	11:35	Bone rearrangement before inurnment No.3	↑ 1	↑ 2
14:50				11:45			
15:00	Cleaning No.2	↑ 2	↑ 4	11:55	Cleaning No.3	↑ 1	↑ 2
15:10				12:40			
15:20				12:50			
15:30				13:10			
15:40				13:20			

(c)				(d)				
Time	Process	OPS	SMPS	Time	Process	OPS	FMPS	LPI
9:10	Cleaning crematory No.2	↑ 1	↑ 5	9:00	Crematory No.3 in operation	↑ 1	↑ 5	↑ 9
9:20	Cleaning No.7	↓ 2	↓ 6	9:30	No.9 in operation			
9:30		↓ 3	↓ 7	10:00	Bone rearrangement No.3	↓ 2	↓ 6	
9:40								
9:50		↑ 4	↑ 8	10:30	Bone rearrangement and cleaning No.9	↑ 3	↑ 7	
12:30								
12:40	Crematory No.3 in operation	↓ 3	↓ 7	12:30	Crematory No. 8, 10 in operation	↓ 4	↓ 8	
12:50								
13:00	After Cremation (No.3)	↑ 4	↑ 8	13:00	Bone rearrangement No.10	↑ 3	↑ 7	
15:00								
15:10				13:30	Bone rearrangement and cleaning No.8	↓ 4	↓ 8	
15:20				14:00				
				15:00				

data for the airborne PM concentrations and their size distributions. Because the process times varied at each crematorium, the exposure was calculated based on the time measured during each process.

Results

Fig. 2 shows the mean of the particle number concentration measured during the working processes of each crematorium. All the mean number concentrations during the working processes (Fig. 2b, c, and d) were higher than the concentrations prior to cremation (Fig. 2a). The concentrations of particle size ranging from 10 to 50 nm increased during the operation process (Fig. 2b). It was assumed that the primary particles associated with combustion were measured. In crematorium B, the maximum particle number concentration during cremation was observed. In the first field survey of crematorium A, the maximum concentration at its peak was >60,000 particles/cm³ (the right side of y-axis in Fig. 2c). During the second field survey, measurements at the time of opening the crematory door could not be conducted because a be-

reaved family was present. Thus, PM was measured after the door was opened. The measured value was lower than that observed in the first survey. The primary particles, which were not detected at other crematoriums during the bone rearrangement process, were detected by opening the door during the crematory’s operation (crematorium A for the second survey in Fig. 2c). Compared with the bone rearrangement process, the peak position of the concentration detected during the cleaning process moved to the right (crematorium A for the first time and crematorium C in Fig. 2d). There is a probability that the residual ash agglomerated during the cleaning process.

Next, the real-time monitoring was analyzed with an emphasis on the maximum concentration measured during the bone rearrangement process in crematorium A in both surveys. Fig. 3 shows the measurement results of the total particle number concentration using SMPS and OPS. High levels of NP number concentrations were measured using SMPS in both surveys immediately after opening the door (Fig. 3a and b). The micron-sized particle concentration measured by OPS did not increase much, but the concentration measured by OPS increased as soon as

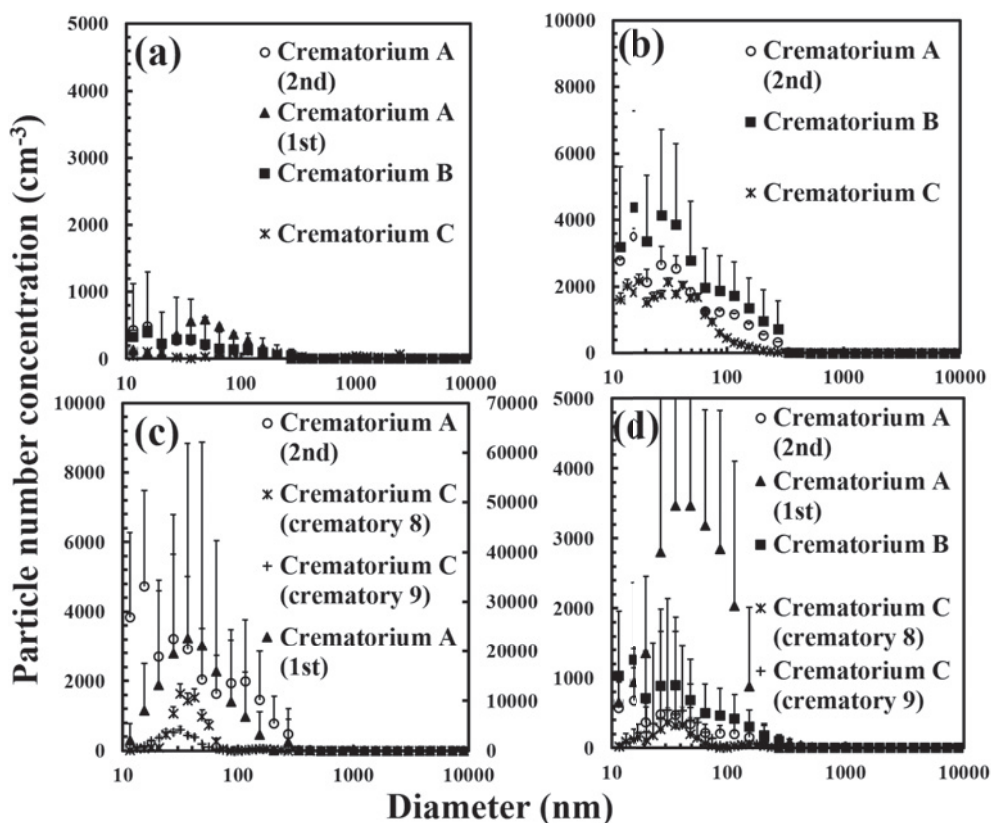


Fig. 2. Mean and SD of the particle number concentration by diameter during each process. (a) Before cremation (crematorium A 1st (n=13), A 2nd (n=24), B (n=17), and C (n=114)), (b) crematorium in operation (crematorium A 2nd (n=17), B (n=11), and C (n=1125)), (c) bone rearrangement time before inurnment; the left side of y-axis for crematorium A second time survey and crematorium C-8 and 9 (crematorium A 2nd (n=17), C-8 (n=120), and 9 (n=259)); the right side of y-axis for crematorium A in the first time survey (crematorium A 1st (n=16)), (d) the cleaning process (crematorium A 1st (n=14), A 2nd (n=22), B (n=22), C-8 (n=249), and 9 (n=431)).

the bone rearrangement operation started. Thus, the concentration measured by OPS was lower than that measured by SMPS, and the peak measured by OPS was detected. The peak proportion measured by OPS during the bone rearrangement process was 300-374 nm particles (Fig. 2c and 3a) and 374-465 nm particles (Fig. 2c and 3b). The scanning delay time of SMPS is longer than that of OPS. Consequently, NPs were estimated to have a longer aggregation time. This could be because of several possibilities. The aggregation of primary particles proceeded for a few minutes after opening the door, or micron-sized dust particles were generated by the bone rearrangement process, or both.

Fig. 4 shows the SEM images of the airborne PM on the filter using LPI. PM showed agglomerates bigger than 10 μm (Fig. 4a). The observed dust was agglomerated by the aggregations of primary particles. The individual particles were nano-sized. EDS was used for elemental mapping of the collected particles. Carbon was the primary component (Fig. 4b). The spectral ratio obtained using

EDS showed two peaks (C and Cl). Because this process eliminated the effect of the blank filter, CK α was detected as the maximum ratio (Fig. 4c). However, the content ratio of heavy metals could not be detected because of limitations of EDS.

Fig. 5 shows the calculation results using the ICRP model and the parameters of the working conditions. Compared with the three respiratory regions, the PM deposition on the alveoli had the highest ratio for diameters ranging from 10 to 300 nm. PM with larger diameters was trapped in the extrathoracic airways. Fig. 5b-e show the calculation results of the total particle deposition number for each respiratory region by working process. The crematorium in operation in Fig. 5b was measured during the first cremation in the morning. In the cremation process, the measurement was temporarily interrupted in crematorium A because a bereaved family entered and left. Therefore, the mean of deposition in measurement time converted to total amount of deposition throughout the whole cremation process by considering the process time.

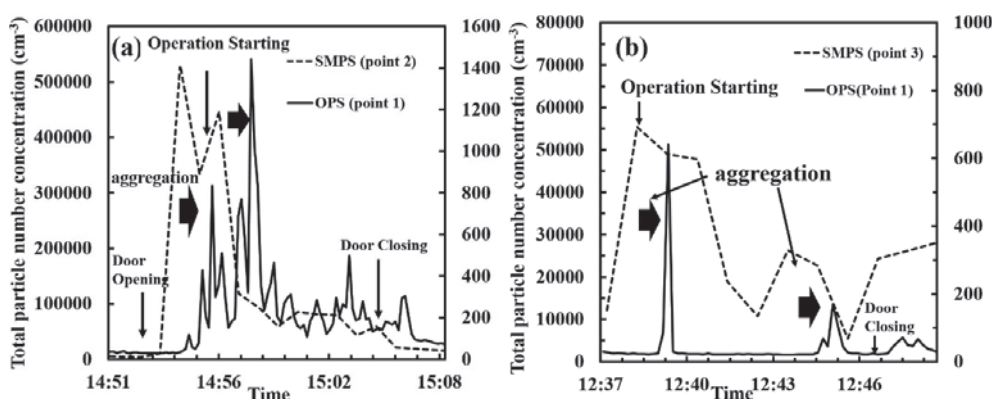


Fig. 3. Real-time total particle number concentration measurements of crematorium A in the first and second surveys using SMPS and OPS during the bone rearrangement process [left (right) side of the y-axis for SMPS (OPS)] for (a) the first and (b) second field survey (Door was opened at a time of 12:35).

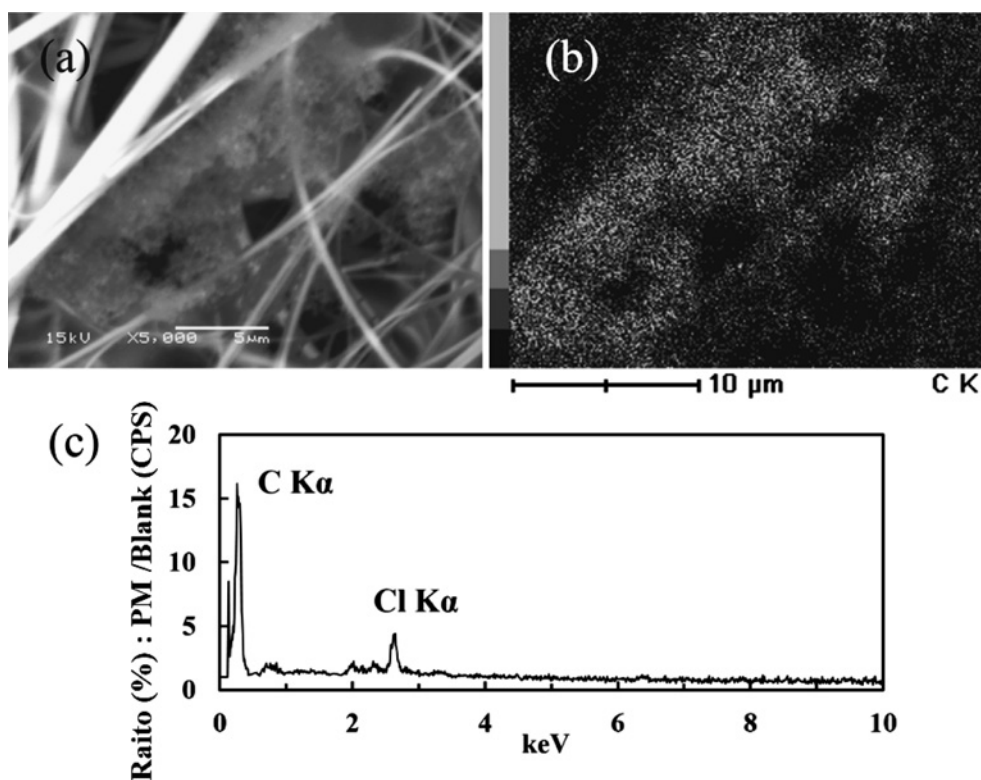


Fig. 4. SEM images of the airborne PM collected by LPI in crematorium C. (a) Airborne PM magnification $\times 5000$, (b) Mapping image of airborne PM (CK α) $\times 5000$, (c) Elemental ratios of collected PM using EDS of SEM.

As several crematoriums were measured in crematorium C, the mean and SD of the depositions during bone rearrangement and cleaning processes are shown in Fig. 5e. Because crematorium C had shorter measuring intervals for the bone rearrangement and cleaning processes than the other crematoriums, it had the lowest exposure per crematory. Focusing on the deposition amount during each working process time by organ using this model, the

deposition in the alveoli during the cremation process was significantly higher than that during the other processes. In contrast, crematorium A during the first survey had the highest exposure. However, the SMPS and OPS data was not collected during cremation because of obstacles. Hence, the maximum exposure was measured during the bone rearrangement process.

Comparing the deposition of alveolar and the other re-

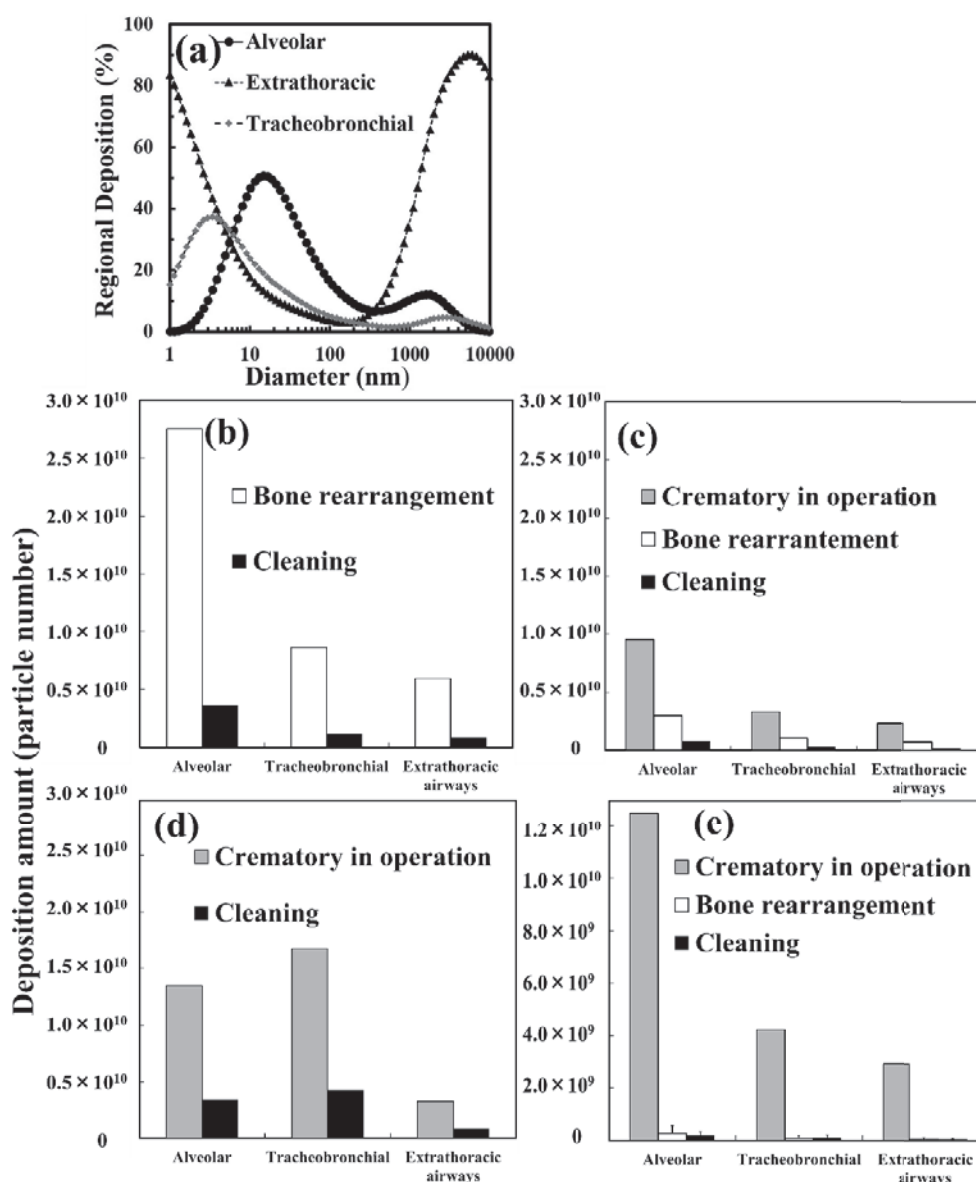


Fig. 5. Function obtained based on the ICRP model (parameters: adult male, light work, and nasal breathing) and total particle deposition in each respiratory region by process. (a) Regional deposition of PM, (b) crematorium A in the first field survey, (c) crematorium A in the second field survey, (d) crematorium B, (e) crematorium C. Bone rearrangement and cleaning are shown as SD of all measured crematoriums ($n=4$).

gions (bb, BB regions and extrathoracic airways) in each investigated crematorium, the ratios (alveolar to the other regions) were 3.2 (bb and BB regions) and 4.6 (extrathoracic airways) for the first survey of crematorium A, 2.9 (bb and BB regions) and 4.1 (extrathoracic airways) for the second survey of crematorium A, 0.8 (bb and BB regions; it is possible that the sample was not working properly because of the obstruction around the inlet of device) and 4.2 (extrathoracic airways) in crematorium B, and 3.0 (bb and BB regions) and 4.3 (extrathoracic airways) in crematorium C. The mean ratios (alveolar to the other regions by a crematorium) were approximately 3.0 (bb

and BB regions, except for the crematorium B) and 4.3 (extrathoracic airways). The ratios were similar for all crematoriums.

Discussion

The maximum of the mean particle number concentration was detected during the bone rearrangement process. Crematorium A, which had the highest concentration, was analyzed the particle number concentration via real-time measurements using SMPS and OPS. The maximum NP number concentration at the time the crematorium's door

opened was 500,000 particle/cm³. However, there is a probability that NPs aggregated into microparticles within a few minutes.

The total particle deposition by each respiratory region during the working processes was based on the ICRP model and was estimated by calculating the particle number concentrations during the working time. Except for crematorium B, which did not conduct a bone rearrangement process, the deposition in the alveoli was the highest compared with all other respiratory regions. Based on the working process time, the highest exposure occurs during the cremation process.

Compared to the deposition during each working process in the same crematorium (crematorium C), the deposition in the alveoli during all working processes was significantly higher than that in the other organs. The functions which obtained using ICRP model calculated under the survey conditions had an alveolar deposition peak at 20 nm (Fig. 5a). Considering the fact that NPs decrease after a few minutes, the exposure to the lungs could be decreased from 500,000 to 100,000 by paying attention to NP exposure at the time the crematory's door opens.

Qualitative analysis of the collected PM samples revealed that carbon was the main component. The second most prevalent element, chlorine, had a peak that was one-third of that of carbon. In the future, tiny amounts of substances such as heavy metals should be analyzed using a high sensitivity device, such as ICP-MS.

The particle number concentration analysis reveals that the particle number concentration in crematorium C was the lowest (Fig. 2). Crematorium C was managed with a pressure control system to prevent the discharge of gases from the crematories. Because the peak distribution of the concentration detected during the cremation process was 10-50 nm, there was a possibility that PM is discharged at some point. However, crematorium C was running three crematories simultaneously during the cremation process. Thus, it is estimated that the deposition during the cremation in crematorium C was less than that in the other crematoriums.

Conclusions

Measurements and calculations from four surveys reveal the inhalation exposure during each working process. In addition, the alveolar exposure during the cremation process was significantly higher than that in other respiratory regions. These results can be applied to estimate the inhalation unit risk of the exposure to each respiratory organ (e.g., lungs and nose) by the additional elemental analysis of NPs. Such estimations could be very useful for health risk assessments.

Acknowledgments: This research was conducted under "Study on reconsideration of the installation management

standard of the crematory" supported by Health Labour Sciences Research Grant.

Conflicts of interest: The authors declare that there are no conflicts of interest.

References

- 1) Mari M, Domingo JL. Toxic emissions from crematoriums: a review. *Environ Int* 2010; 36: 131e137.
- 2) Xue Y, Tian H, Yan J, Wang K. Present and future emissions of HAPs from crematoriums in China. *Atmos Environ* 2016; 124: 28-36.
- 3) The Ministry of Health, Labour and Welfare. Public Health Administration Report. [Online]. 2015. Available from: URL: <http://www.e-stat.go.jp/SG1/estat/List.do?lid=000001162868> [in Japanese]
- 4) Takeda N, Takaoka M, Fujiwara T, Takeyama H, Eguchi S. PCDD/Fs emissions from crematoriums in Japan. *Chemosphere* 2000; 40: 575-586.
- 5) Takeda N, Takaoka M, Fujiwara T, Takeyama H, Eguchi S. Measures to prevent emissions of PCDD/Fs and co-planar PCBs from crematoriums in Japan. *Chemosphere* 2001; 43: 763-771.
- 6) Wang LC, Lee WJ, Lee WS, Chang-Chien GP, Tsai PJ. Characterizing the emissions of polychlorinated dibenzo-p-dioxins and dibenzofurans from crematoriums and their impacts to the surrounding environment. *Environ Sci Technol* 2003; 37: 62-67.
- 7) Mills A. Mercury and the crematorium chimneys. *Nature* 1990; 346: 615.
- 8) Basu MK, Wilson HJ. Mercury risk from teeth. *Nature* 1991; 349: 109.
- 9) Kunzler P, Andree M. More mercury from crematoria. *Nature* 1991; 349: 746-747.
- 10) Hogland W. Usefulness of selenium for the reduction of mercury emission from crematoria. *J Environ Qual* 1994; 23: 1364-1366.
- 11) Yoshida M, Kishimoto T, Yamamura Y, Tabuse M, Akama Y, Satoh H. Amount of mercury from dental amalgam filling released into the atmosphere by cremation. *Japanese J Public Health* 1994; 41: 618-624 (in Japanese).
- 12) Takeda N, Takaoka M, Oshita K. Measures to prevent emissions of hazardous materials from crematoriums in Japan. *Environ Eng Res* 2008; 45: 259-270 (in Japanese).
- 13) Takeda N, Takaoka M, Oshita K, Eguchi S. Measures and source to prevent emissions of hexavalent chromium compounds in ash from crematoriums in Japan. *Environ Eng Res* 2008; 45: 259-270 (in Japanese).
- 14) Oshita K, Takaoka M, Eguchi S, Shiota K. Behavior of acidic gas, mercury and fine particles emitted from a crematorium. *EICA* 2012; 17: 116-125 (in Japanese).
- 15) Oshita K, Takaoka M, Eguchi S, Shiota K. Behavior of acidic gas, mercury and fine particles emitted from a crematorium-part 2. *EICA* 2013; 18: 32-41 (in Japanese).
- 16) Takaoka M, Oshita K, Takeda N, Morisawa S. Mercury emis-

- sion from crematoriums in Japan. *Atmos Chem Phys* 2010; 10: 3665-3671.
- 17) Nieschmidt AK, Kim ND. Effects of mercury release from amalgam dental restorations during cremation on soil mercury levels of three New Zealand crematoria. *Bull Environ Contam Toxicol* 1997; 58: 744-751.
 - 18) Santarsiero A, Settimo G, Dell'andrea E. Mercury emission from crematoria. *Ann Ist Super Sanita* 2006; 42: 369-373.
 - 19) Maloney SR, Phillips CA, Mills A. Mercury in the hair of crematoria workers. *Lancet* 1998; 352: 1602.
 - 20) Oberdörster G, Sharp Z, Atudorei V, et al. Extrapulmonary translocation of ultrafine carbon particles following whole-body inhalation exposure of rats. *J Toxicol Environ Health A* 2002; 65: 1531-1543.
 - 21) Grassian VH, O'shaughnessy PT, Adamcakova-Dodd A, et al. Inhalation exposure study of titanium dioxide nano-particles with a primary particle size of 2 to 5 nm. *Environ Health Perspect* 2007; 115: 397-402.
 - 22) The International Commission on Radiological Protection (ICRP). ICRP Publication 66: Human respiratory tract model for radiological protection. *Annals of the ICRP* 1994; 24: 1-300.

Journal of Occupational Health is an Open Access article distributed under the Creative Commons Attribution-NonCommercial-ShareAlike 4.0 International License. To view the details of this license, please visit (<https://creativecommons.org/licenses/by-nc-sa/4.0/>).